Mathematical Modeling of Induced Foreign Protein Production by Recombinant Bacteria

Jongdae Lee and W. Fred Ramirez*
Department of Chemical Engineering, University of Colorado, Boulder, Colorado 80309-0424

Received February 27, 1991/Accepted September 27, 1991

A new generalized mathematical model for recombinant bacteria which includes inducer effects on cell growth and foreign protein production is developed. The model equation set was applied to a host–vector system, *Escherichia coli* D1210 and plasmid pSD8. Batch experiments were designed and performed in shake flasks to verify the model. A parameter estimation method was developed and proven to be efficient. Although simple, the model can effectively describe the dynamics of the production of foreign protein in recombinant bacteria and can be used for optimization and control studies to maximize foreign protein production.
Key words: induced protein • mathematical modeling • recombinant bacteria

INTRODUCTION

There has been significant research in the effort to describe the dynamics of foreign protein production in recombinant bacteria.[5,6,14,16] Complex structured models[3,11,13] have been developed to give detailed knowledge of intracellular components. But these models are too complicated to use for optimization and control studies. Previous unstructured models[1,15] were too simple in that they could not include the effect of an inducer on protein production as well as the influence of the inducer on cell growth rate.

One of the eventual goals in the study of recombinant bacteria is to maximize the production of useful foreign protein by exploiting the host cell's metabolism. Even though well-formulated structured and unstructured models have been developed, none of them are appropriate as a model for applying optimal control theory in order to get optimal control laws for the maximum production of foreign protein. This is mainly due to lack of parameter information, their use of complex intracellular phenomena, and the fact that the models result in nonobservable systems. Abundant quantitative and qualitative kinetic data for the glucose effect on specific growth rate are now available. But there are not sufficient data concerning the inducer effect on specific growth rate and foreign protein production. We develop and experimentally test a mathematical model which includes the inducer effect on specific growth rate and foreign protein production.

* To whom all correspondence should be addressed.

Even though most of the major macromolecular events involved in the amplification of the production of a foreign gene inserted into plasmids are elucidated, a simple adequate quantitative description of the interactions among host cell's metabolism, inducer level, and the foreign gene expression rate needs to be formulated. Considerable kinetic data for the inducer effect on specific growth rate have been obtained from the previous work of Bentley.[2] In Bentley's work, a structured model set was developed which can describe the formation and depletion of the macromolecules and the constituent metabolites. A major advantage of the model is that all kinetic equations contain physically meaningful terms based on cellular biochemistry. Efforts to add biochemical meanings into the model structure are usually accompanied by a large number of unevaluatable parameters, leading to lack of confidence as well as the lack of observability of the model. Our past experience in process optimization with biochemical processes[9] demonstrates the importance of developing an applicable model set which, even though it may lack some of the structural meaning, can lead to the solution of an optimal operation strategy without loss of the generality. The idea is to capture an accurate yet simple description of the major operable mechanisms. With the knowledge of any *Escherichia coli* cloned protein expression system, which has been accumulated during the last several years, and the understanding of the specific plasmid and host *E. coli* system, which is chosen to be representative and will be used in our experimental work, a model framework is built with detailed functional structure. Naturally, however, in the process of molding the library of information into an adequate, applicable model equation set, some of the detailed kinetics or dynamics are expected to be lumped into simple mathematical forms. Consequently, a set of experiments need to be designed to identify part of the resultant model structure and the kinetic parameters which have become uncertain through this lumped modeling procedure.

Recent work has pointed out the importance of nutrient concentration and inducer level of foreign protein production. It was demonstrated that a high inducer level could result in higher production of foreign protein in a cell but could reduce the cell growth rate signifi-

Biotechnology and Bioengineering, Vol. 39, Pp. 635–646 (1992)

CCC 0006-3592/92/060635–012$04.00

cantly. Experimental results of this work shows that the specific growth rate changes with time after induction (Fig. 7). Any model needs to include this dynamic effect of inducer level on specific growth rate.

Inducer injection time was also shown to be an important factor in maximizing the production of foreign protein. Bentley[2] and Park and co-workers[10] showed that an optimal injection policy of inducer to induce foreign protein production in bacteria might exist for a given operational period. Early injection may result in small numbers of cells at final time because of the negative effect of inducer on cell growth rate when a host–vector system is influenced significantly by inducer level. Late injection may cause a small amount of protein level in a cell when the foreign protein is not induced strongly in a host–vector system.

Different host–vector systems are influenced differently by inducer injection. This article develops a new mathematical model which can describe this phenomena effectively and is simple enough to be effective for optimization and control studies.

SPECIFIC GROWTH RATE

Because specific growth rate is a function of time, nutrient level, and inducer level, the following equation can be formulated:

$$\mu = \mu(t, C_N, C_I) \tag{1}$$

where C_N is nutrient level and C_I is inducer level.

Before we propose our model, we assumed that there are three types of host–vector systems.

Type I: After inducer injection, the specific growth rate does not change significantly.

Type II: After inducer injection, the specific growth rate decreases sharply due to the metabolic burden to cell, but later recovers from the inducer shock.

Type III: After inducer injection, the specific growth rate decreases monotonically.

Figure 1 represents the three types of response graphically. To cover all three types, we develop a model for type II behavior, since types I and III are extremal cases of type II, i.e., type I has no shock term and type III has no significant recovery term.

Figure 2 shows that the specific growth rate for a type II system was constructed as the sum of a shock term and a recovery term. The proposed equation for the specific growth rate is

$$\mu = \frac{\mu_{\max} C_N}{K_{C_N} + C_N}(k_s + k_r R_R) \tag{2}$$

where k_s is the shock rate effect, k_r is the recovery rate effect, and R_R is the recovery ratio. The recovery ratio is defined as the ratio of the specific growth rate at an inducer concentration to the maximum specific growth rate $\mu_{\max}$. The constants $\mu_{\max}$ and K_{C_N} are Monod model parameters that describe the effect of nutrient level on the specific growth rate.

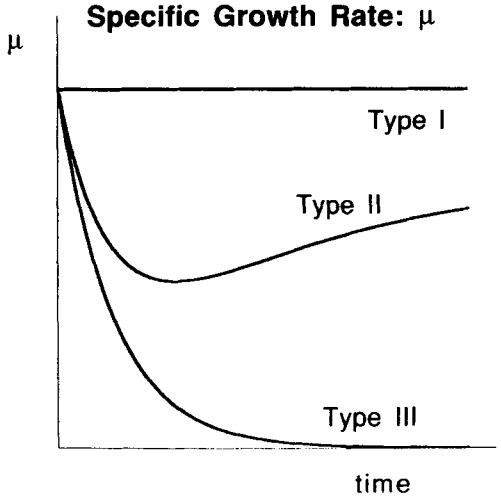

Figure 1. Possible inducer effects on specific growth rate.

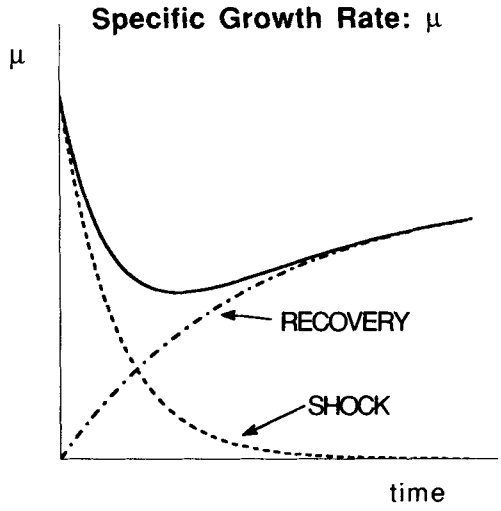

Figure 2. Specific growth rate as a sum of shock and recovery effects of induction.

We model the shock and recovery dynamics by first-order kinetic expressions:

$$\frac{dk_s}{dt} = -k_1 k_s \qquad k_s(0) = 1 \tag{3}$$

$$\frac{dk_r}{dt} = k_2(1 - k_r) \qquad k_r(0) = 0 \tag{4}$$

Here the rate parameters k_1 and k_2 are assumed to be functions of inducer concentration and are described by Monod expressions:

$$k_1 = \frac{k_{11} C_I}{K_{IX} + C_I} \tag{5}$$

$$k_2 = \frac{k_{22} C_I}{K_{IX} + C_I} \tag{6}$$

where k_{11} and k_{22} are constants which determine the rates of shock and recovery, respectively, and K_{IX} is a Monod-type constant. The recovery ratio R_R must be determined by experimentation and is a function of

the inducer concentration. The functional form considered is

$$R_R = \frac{A}{A + C_I} \tag{7}$$

where A is a constant to be determined from experimentation.

FOREIGN PROTEIN PRODUCTION RATE

Another important factor in modeling foreign protein production is the foreign protein production rate R_f. Here we assume that R_f is a function of inducer and nutrient levels. At a high level of inducer concentration, experimental data show saturation phenomena for foreign protein production (Fig. 3). Based upon the data of Figure 3, we propose the following functional form:

$$R_f = \left(\frac{f_{\max} C_N}{K_{C_N} + C_N}\right)\left(\frac{f_{I_O} + C_I}{K_I + C_I}\right) \tag{8}$$

where $f_{\max}$ and K_I are Monod-type constants. This is a model that shows Monod kinetics as a function of nutrient level C_N and inducer concentration C_I. The last term is a modified Monod expression introducing the constant f_{I_O}. This is needed because the cells will produce foreign protein without inducer present.

A NEW MATHEMATICAL MODEL

Our mathematical model for the fed-batch production of foreign protein with induction is given below:

$$\dot{V} = q_N + q_I \quad \text{(total material balance)} \tag{9}$$

where q_N is the nutrient feeding rate (L/h) and q_I is the inducer feeding rate (L/h);

$$\dot{X} = \mu(t, C_N, C_I)X - \frac{q_N + q_I}{V} X \quad \text{(biomass balance)} \tag{10}$$

where X is the cell density (g/L) and $\mu(t, C_N, C_I)$ is the specific growth rate (h^{-1});

$$\dot{C}_N = \frac{q_N}{V} C_N^f - \frac{q_N + q_I}{V} C_N - \frac{\mu(t, C_N, C_I)}{Y(C_N, C_I)} X$$

(nutrient material balance) (11)

where C_N is the nutrient concentration (g/L) and $Y(C_N, C_I)$ is the growth yield coefficient (the yield coefficient is considered as a constant in this work although it can be a function of both nutrient and inducer concentration for some systems);

$$\dot{C}_P = R_f(C_N, C_I)X - \frac{q_N + q_I}{V} C_P$$

(foreign protein material balance) (12)

where C_P is the foreign protein concentration (g/L) and R_f is the protein synthesis rate (h^{-1}); and

$$\dot{C}_I = \frac{q_I}{V} C_I^f - \frac{q_N + q_I}{V} C_I$$

(inducer material balance) (13)

where C_I is the inducer concentration (g/L).

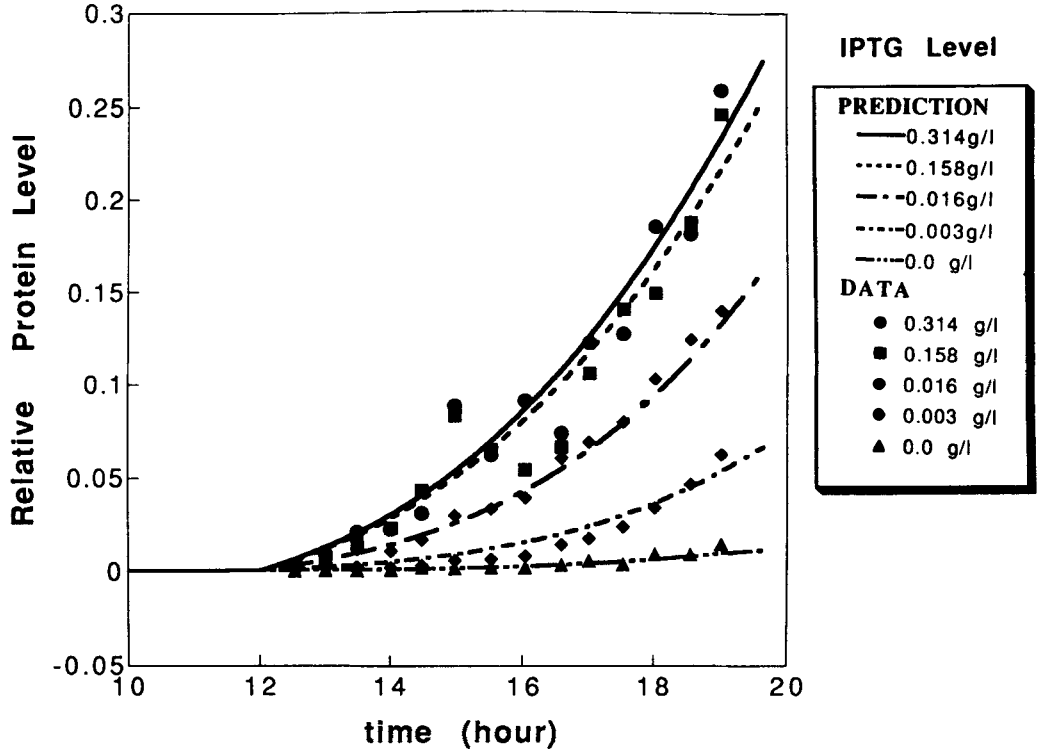

Figure 3. Effect of IPTG concentration on β-galactosidase protein production. Experimental data and model predictions.

EXPERIMENTAL WORK

Batch experiments were performed in shake flasks to verify the proposed model with *E. coli* D1210 and plasmid pSD8.[7] The D1210 strain has a genotype, F^-, *lac*(i^a, o^+, z^+, y^+), gal^-, pro^-, leu^-, thi^-, $endoI^-$, *hsm*, *hsr*, *recA*, *rpsL*. The pSD8 plasmid has the same structure as pBC26 with two changes. The Pra2 promoter is replaced by the tacII promoter, and the ribosom binding site and initiation codon are inserted between the BglII and PstI sites.[4] Proline, leucine, and thiamine were added to M9 minimal media. Ampicillin (100 μM/mL) was used to remove plasmid-free cells. Isopropylthiogalactoside (IPTG) was used as the inducer. The produced protein is β-galactosidase, which hydrolyzes β-D-galactosides. The enzyme can hydrolyze colorless *o*-nitrophenyl-β-D-galactoside (ONPG). Since the produced *o*-nitrophenol is yellow, the relative protein levels can be measured by absorption spectrometry at 420 nm. The relative protein level is defined as the ratio of an optical measurement of the produced *o*-nitrophenol to that of a standard solution without any *o*-nitrophenol. The approximate protein levels can be calculated by comparing with a standard β-galactosidase.

Sodium dodecyl sulfate–Polyacrylamide gel electrophoresis (SDS–PAGE) of the protein gave qualitative data on the protein dynamic response after induction (Fig. 4). Since the β-galactosidase is a relatively large protein (monomer 116 kD), a 5% acrylamide concentration was used. The gel was very fragile. Samples were taken at a 30-min interval and then put into an ice bath. The gel electrophoresis results of Figure 4 showed that there was definitely an effect of inducer level on protein production for this system.

In order to develop quantitative data, the following experimental procedure was developed. A volume of 400 mL of sterilized media was inoculated with overnight culture which was inoculated the previous day to ensure that the cells are in the exponential growth phase. After the optical density reached 0.1, the media was divided into five 250-mL sterilized beaker flasks, and a different amount of inducer was injected into each beaker flask. Samples of 4 mL were taken at 30-min intervals from each beaker flask and stored in an ice bath. A 2-mL sample of the media was then used for optical density measurement by absorption spectrometry at 600 nm to determine cell mass. A 1-mL sample of the media was sonicated inside an ice bath using a W-380 sonicator by Heat Systems–Ultrasonics and then put into a freezer for next-day protein assay. The optimal sonication time was 1.5 min at a 50% load of operation (Fig. 5). This is the minimum time which allowed for consistent results. The data with 0.5 min sonication time were not consistent when compared to those with longer sonication times. Sonication time of 1.5 min was appropriate to continue sampling work at each 30-min interval. Finally, 1 mL of media was spinned to remove the cells in order to prepare samples for next-day glucose assay.

PARAMETER ESTIMATION

Determination of Specific Growth Rate Model Parameters

The specific growth rate model parameters μ_{max} and K_{C_N} were determined from experimental growth data without IPTG. While the state equations were integrated, the differences between experimental data and simulation data of optical density at each sampling time were calculated and the sum of squares error (SSE) for each value set of μ_{max} and K_{C_N} were compared to get best values. From the data without IPTG, the Monod parameters were determined as $\mu_{max} = 0.41\ h^{-1}$ and $K_{C_N} = 0.108$ with a SSE of 0.0019. Since there were 14 points, the average error for each data point was 0.012, which implies 1.85% error compared to the average optical density of experimental data without any

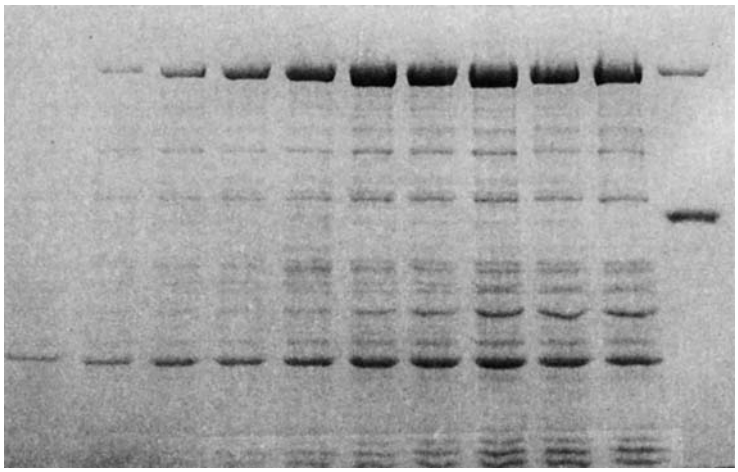

Figure 4. β-Galactosidase production by gel electrophoresis as a function of production time.

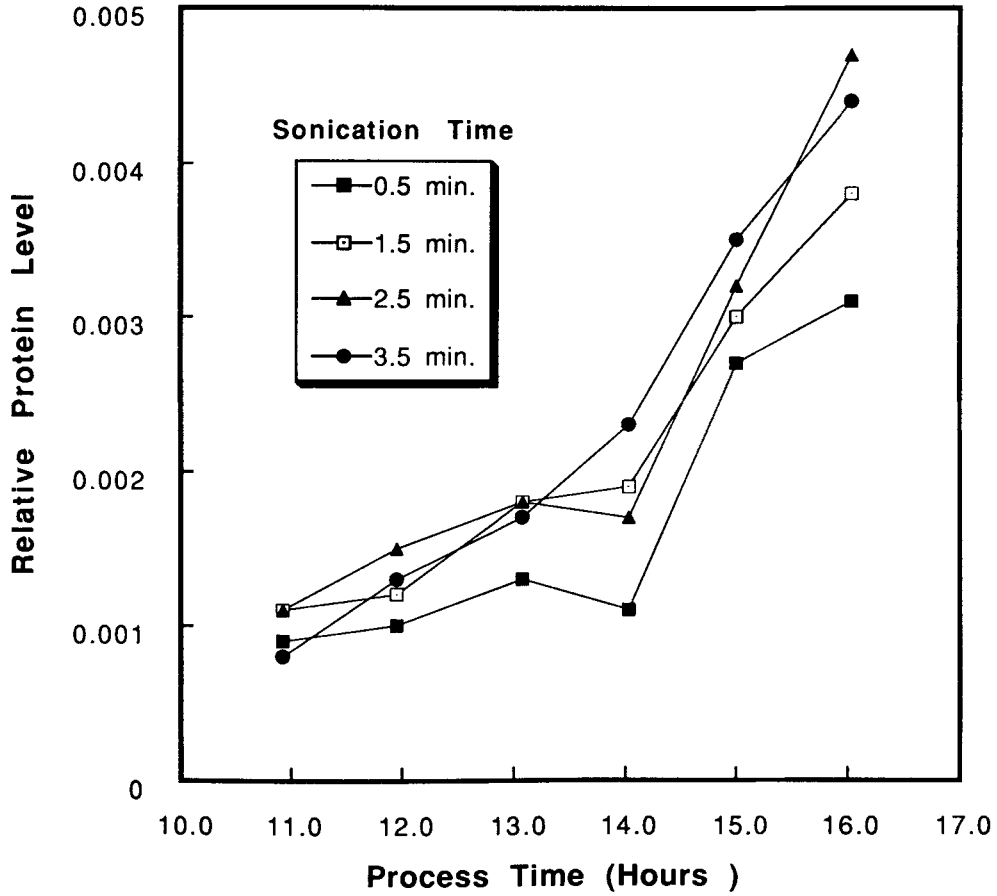

Figure 5. Effect of Sonication time on protein assay.

IPTG. Figure 10 (0 g/L IPTG) shows the simulated responses as well as the experimental data.

The recovery ratio R_R is determined from specific growth rate data at the final experimental time. For a batch system, optical measurement of cell mass is described by

$$\frac{dX^O}{dt} = \mu(t, C_N, C_I)X^O \tag{14}$$

where X^O is optical density.

To get values of μ at each sampling time, the graph of $\ln(X)$ vs. t is needed and μ is the slope of the graph at each sampling time. However, this method is very sensitive to experimental error and is not a satisfactory technique. Therefore, an alternate method was used. First, the optical density data are fit using third-order polynomial equations as shown in Figure 6. The polynomial equations are inserted into Eq. (14) to get μ values directly. The resulting specific growth rates as a function of time and inducer concentration are shown in Figure 7. There are two main error sources in Figure 7. First for small beaker flask experiments the optical densities increase when IPTG is injected. Another error comes from use of the third-order polynomial regression of the optical density data.

For *E. coli* D1210 and plasmid pSD8, the recovery ratio function of inducer level of Eq. (7) was assumed. The least squares parameter fit for this system is A = 0.22 g/L using the IMSL nonlinear regression routine, RNLIN.[12] The SSE is 0.0066. Figure 8 shows both the experimental data and model simulation of the recovery ratio as a function of IPTG level. The average error in the fit is 5.2%. Figure 9 shows the shock and recovery terms for our experimental system when the IPTG level is 0.0159 g/L.

Since the specific growth rate, the slopes in Figure 10, can be described by a monotonically decreasing function at all IPTG levels, we assumed that the shock rate constant k_1 is equal to the recovery rate constant k_2 in Eqs. (3) and (4).

Using the experimental data of Figure 10, the parameters k_{11} and K_{IX} of Eq. (5) were determined by a least squares method. While the state equations for growth are integrated, the SSE between experimental data and simulation data of optical densities are compared to determine the best k_1 value for each IPTG concentration level. Once the shock rate constant k_1 is known, the parameters k_{11} and K_{IX} of Eqs. (5) and (6) were determined using the IMSL nonlinear regression routine, RNLIN.[12] The Monod-type constants were determined as k_{11} = 0.09 h^{-1} and K_{IX} = 0.034 g/L. The residual SSE between experimental and simulation data of optical densities is 0.09. Since there are 65 data points, an average error per data point is 0.037, which implies 6.9% error

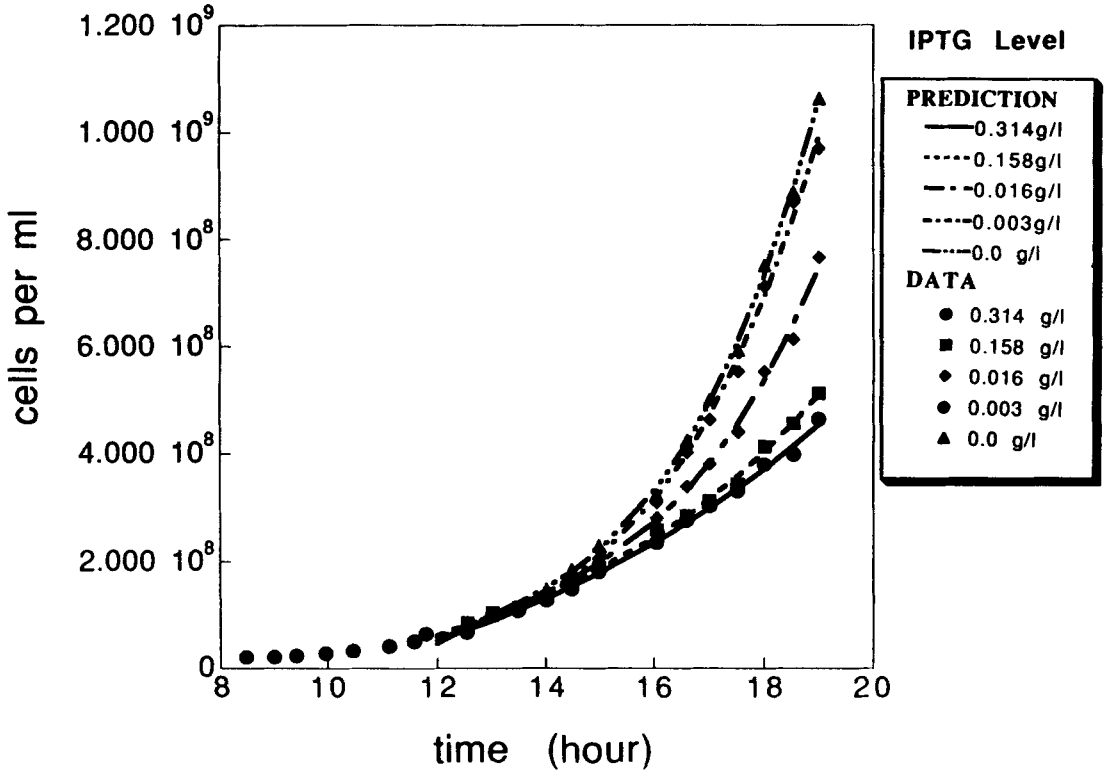

Figure 6. Effect of IPTG concentration on cell growth. Experimental data and third-order polynomial regression fits.

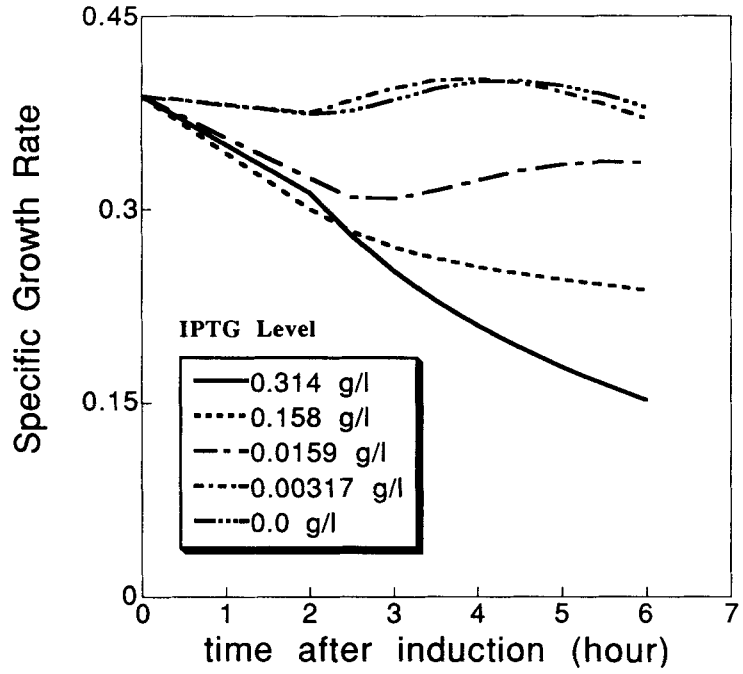

Figure 7. Specific growth rates from the experimental data. Results of third-order polynomial fits.

per data point compared to the average optical density of experimental data. Figure 10 shows the comparison of the final growth model at different inducer concentration levels. This model has therefore effectively simulated the effect of inducer concentration on the growth response.

Determination of the Protein Production Rate Constants

Five sets of relative protein level data at different inducer concentrations (Fig. 3) were used to determine production rate parameters $f^O_{\max}$, K_I, and F_{I_O}. The variable $f^O_{\max}$ is defined as $f_{\max}X_c/P_c$, where P_c is a propor-

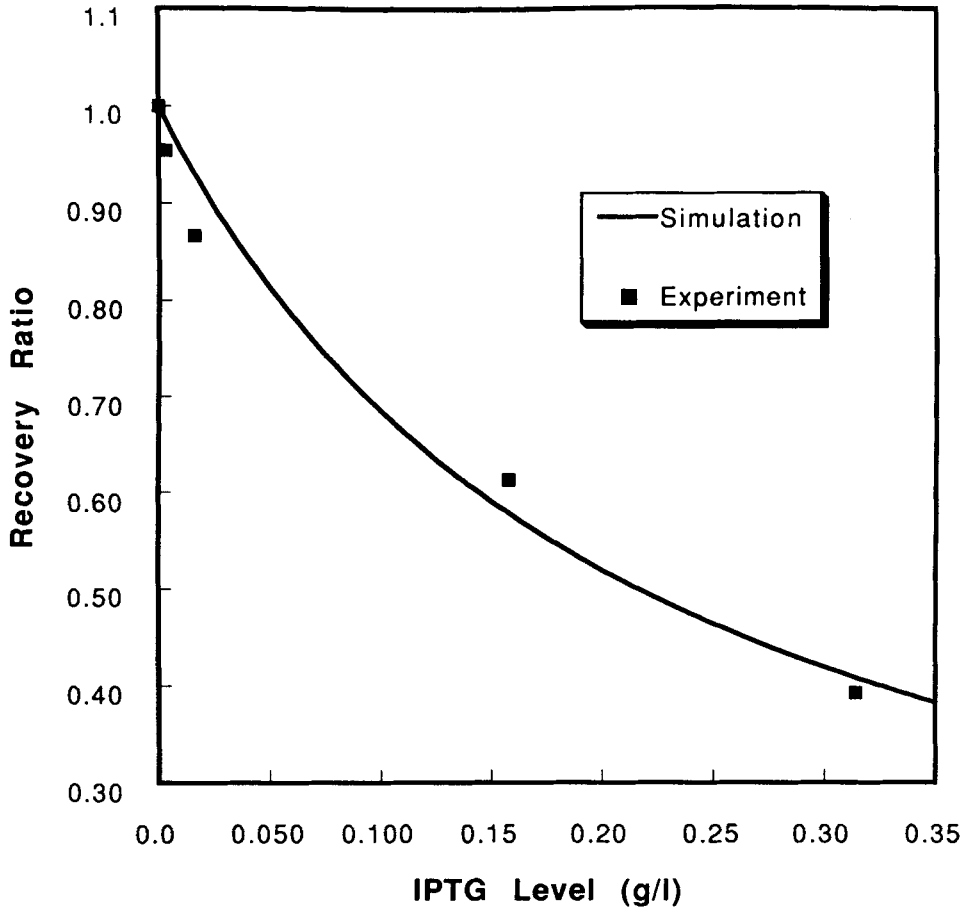

Figure 8. Recovery ratio as a function of IPTG concentration. Experimental data and simulation results.

tional ratio of protein level, C_P, to the relative protein level, C_P^o, and X_c is a proportional ratio of the cell mass, X, to optical density, X^o. The protein production rate [Eq. (8)] becomes

$$R_f^o = \frac{f_{\max}^o C_N}{K_{C_N} + C_N} \frac{f_{I_O} + C_I}{K_I + C_I} \tag{15}$$

At each level of inducer concentration, the production rate R_f^o is a constant and increases with inducer concentration. Least squares regression yielded a best fit of the reaction rate R_f^o as a function of inducer concentration. Figure 3 shows the actual protein data and the simulated data. Dimensionless relative protein level was used to get parameters in Eq. (15) rather than protein level in grams per liter. The values of R_f^o were determined for each IPTG concentration using the least squares method. Once the production rate R_f^o is known, the parameters $f_{\max}^o$ and K_I of Eq. (15) were determined using the IMSL nonlinear regression routine, RNLIN.[12] The best fit values are $f_{\max}^o = 0.095\ h^{-1}$, $f_{I_O} = 0.0005$ g/L, and $K_I = 0.022$ g/L with a SSE between the actual protein data and the simulated data of 0.0094. Since there are 70 data points, an average error per data point is 0.012, which implies a 23.2% average error compared to the average relative protein level of experimental data. The relatively large error is mainly due to the scatter in the data at higher inducer levels. Figure 3 shows relative protein levels of both the actual experimental data and the model simulation data as a function of inducer concentration.

Simulation

The model equation set for fed-batch operation was integrated with different glucose and inducer feeding policies. The unit for cell mass is dimensionless since we use optical density as the variable. The actual cell mass can be calculated from optical density.[8] The unit for protein level is also dimensionless, since it is relative protein level. The simulation results are shown in Figure 11. Two cases with different feeding policies were considered. For case 1, the glucose feeding rate is 10 mL/h and the IPTG feeding rate is 0.1 mL/h throughout the operation. For case 2, the glucose feeding rate is 10 mL/h throughout the operation and the IPTG feeding rate is 100 mL/h for the first 2.4 min and 0.1 mL/h throughout the rest of the operation. The initial and final values of the state variables of a fed-batch operation simulation for both cases are shown in Table I. From Figure 11, (part 11.1) we can see that the cell mass increase is less for case 2 with higher IPTG concentration because of IPTG inhibition effect on cell growth. Nev-

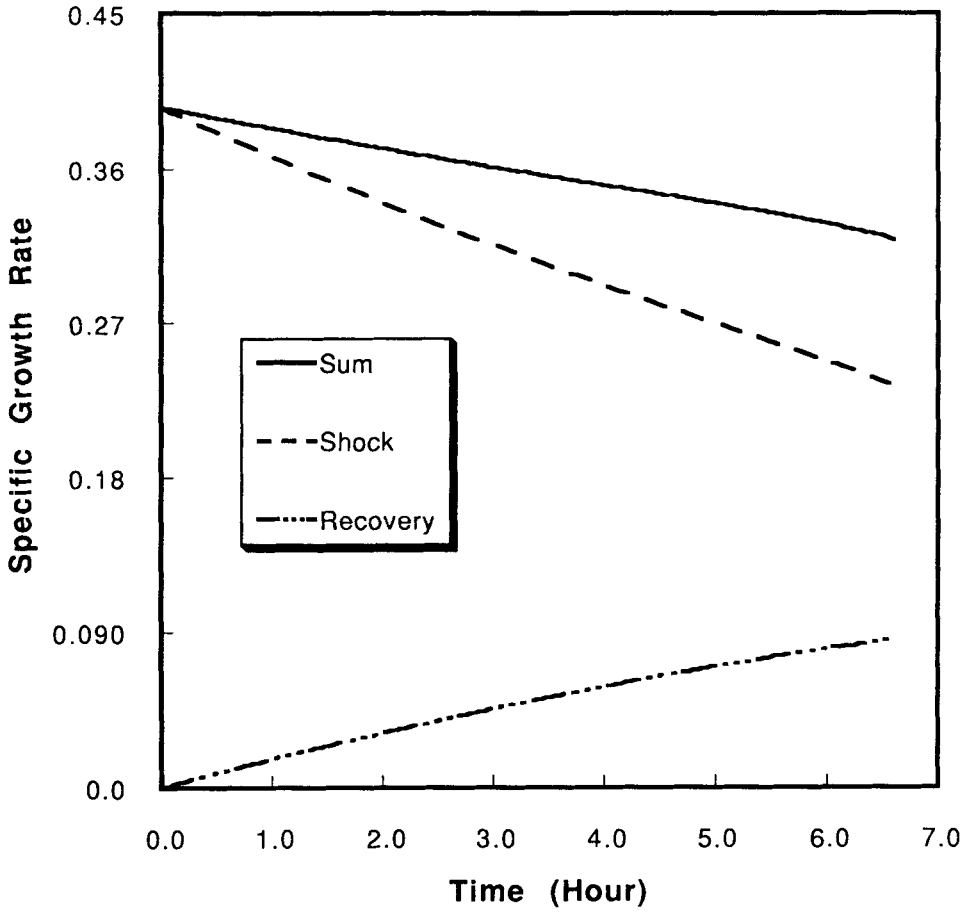

Figure 9. Specific growth rate as a sum of shock and recovery effects for the experimental system studied.

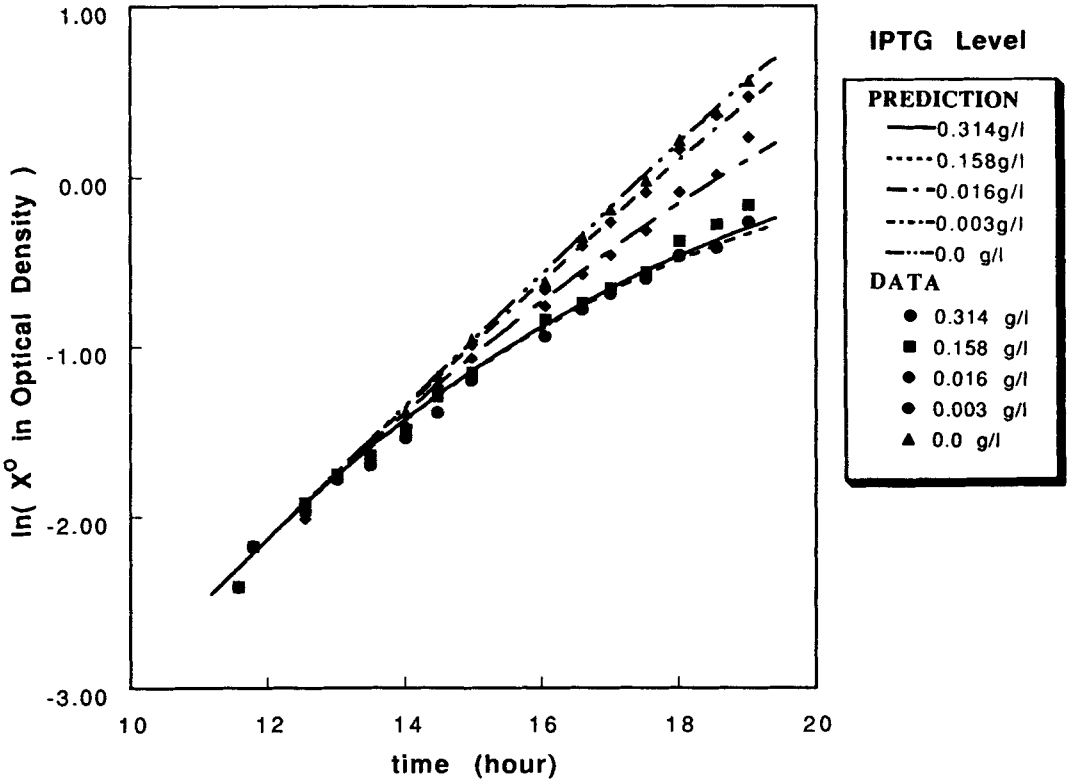

Figure 10. Effect of IPTG concentration on cell growth. Experimental data and simulation results.

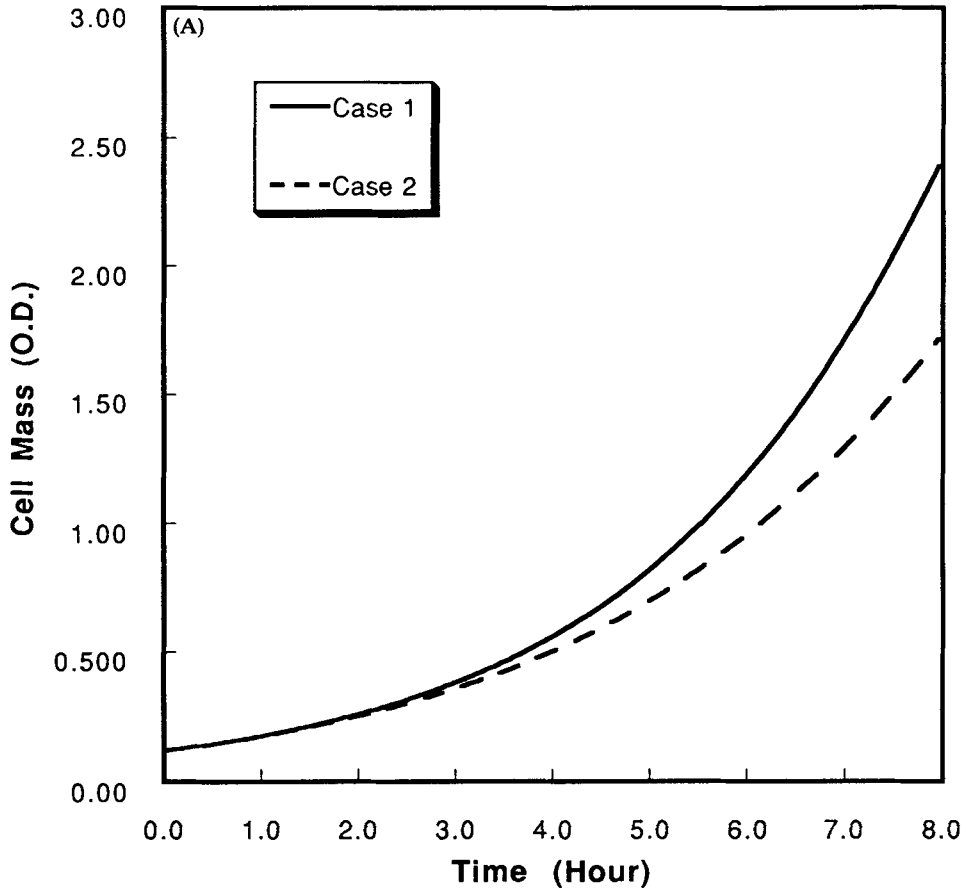

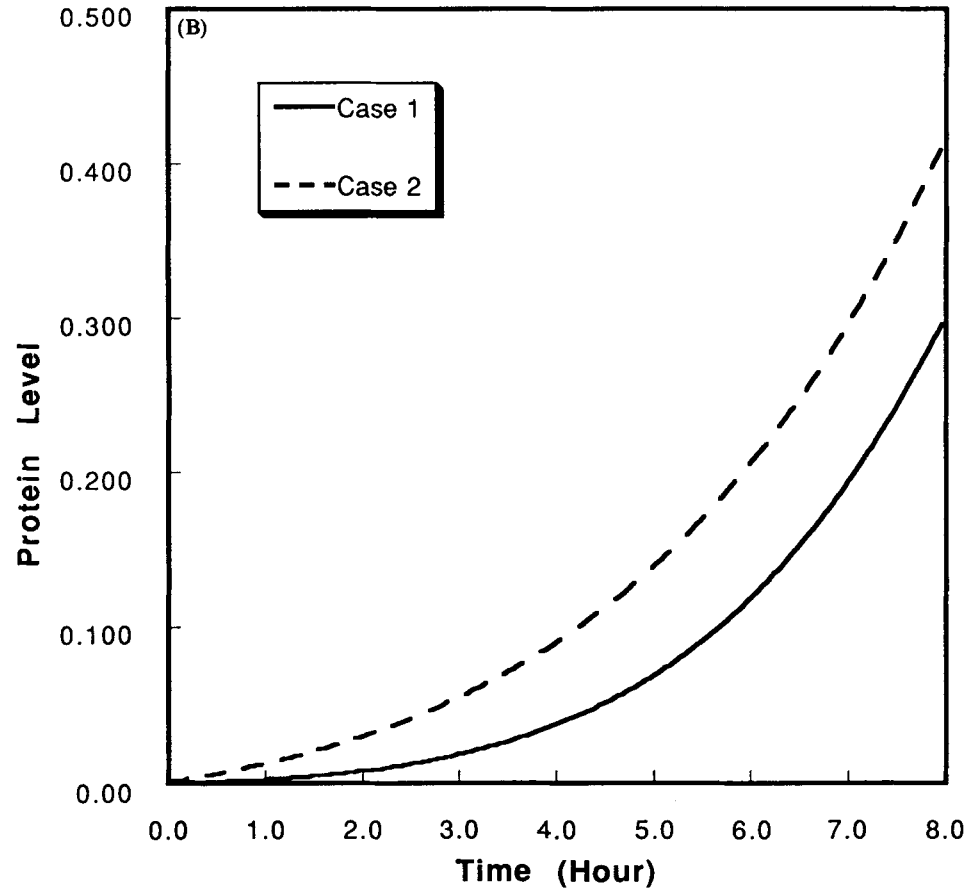

Figure 11. Fed-batch bioreactor simulation results. (A) *Case 1:* Glucose feed rate of 10 mL/h and IPTG feed rate of 0.1 mL/h throughout the operation. (B) *Case 2:* Glucose feed rate of 10 mL/h throughout the operation and IPTG feed rate of 100 mL/h for first 2.4 min and 0.1 mL/h for rest of operation. (11.1) Cell mass vs. time. (11.2) protein levels vs. time.

Table I. Initial and final state variables under fed-batch operation.

State variables	Initial values	Final values	
		Case 1	Case 2
Volume (L)	1.0	1.08	1.084
Cell mass (OD)	0.12	2.39	1.716
Glucose concentration (g/L)	3.82	0.547	1.847
Relative protein level (OD)	0.00087	0.296	0.412
IPTG concentration (g/L)	0.	0.037	0.221

ertheless case 2 produced more protein (part 11.2) because the IPTG effect on protein production is relatively greater than the IPTG effect on cell growth inhibition.

APPLICATION TO OPTIMIZATION OF BATCH SYSTEMS

When the glucose and the inducer feeding rates are zero, the system becomes that of a batch culture. We assume that the inducer is injected as an impulse. To get the inducer input time and inducer input amount that maximizes the foreign protein production, the model equation set was integrated with different injection times and inducer levels. From Figure 12, we can see that earlier injection is better for our host–vector system. Once a critical amount of IPTG is injected, its sensitivity to improve protein production is limited. Due to this decrease in production sensitivity, there will exist optimal injection time and amount of inducer for a batch system depending on the price of inducer. This is due to the fact that the inducers such as IPTG are very expensive. The optimal strategy for our experimental system to maximize the profit from the foreign protein production is that the earlier injection is the better and the amount of inducer depends on the price of inducer considering the production sensitivity.

DISCUSSION AND CONCLUSIONS

The introduction of the new state variables k_s of Eq. (3) and k_r of Eq. (4) can explain the effect of inducer concentration on cell growth rate effectively. From Figure 6, two extremes in cell growth with inducer concentration can be observed. One is the maximum growth rate without any inhibition and the other is the minimum growth rate with full inhibition. These phenomena are modeled by the shock and recovery concept of Figure 2 and are described mathematically by the first-order kinetic properties of Eqs. (3) and (4) and the recovery ratio of Eq. (7). The most promising aspect of this modeling work is that any kind of growth rate inhibition can be expressed by modifying the recovery ratio function and the shock and recovery parameters appropriately. It is also possible to add additional conceptual characteristics to the specific growth rate model [Eq. 2] such as protein inhibition.

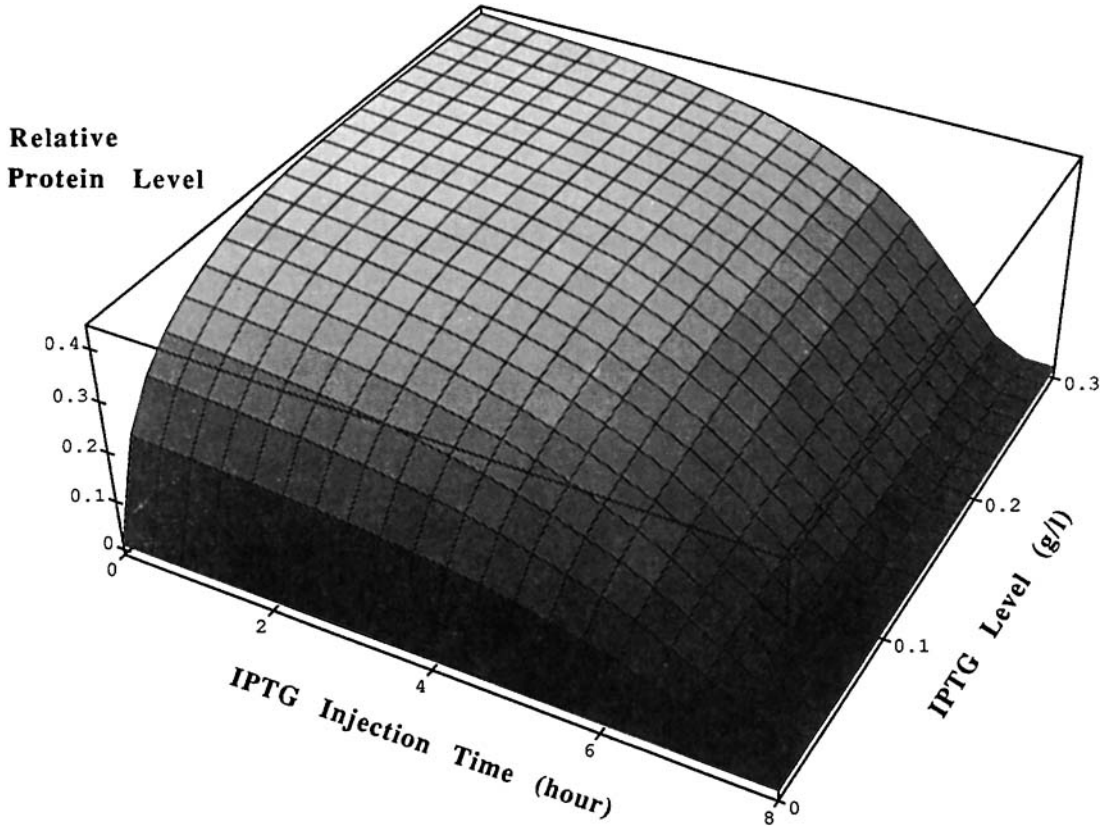

Figure 12. Protein production with various IPTG levels and IPTG injection times.

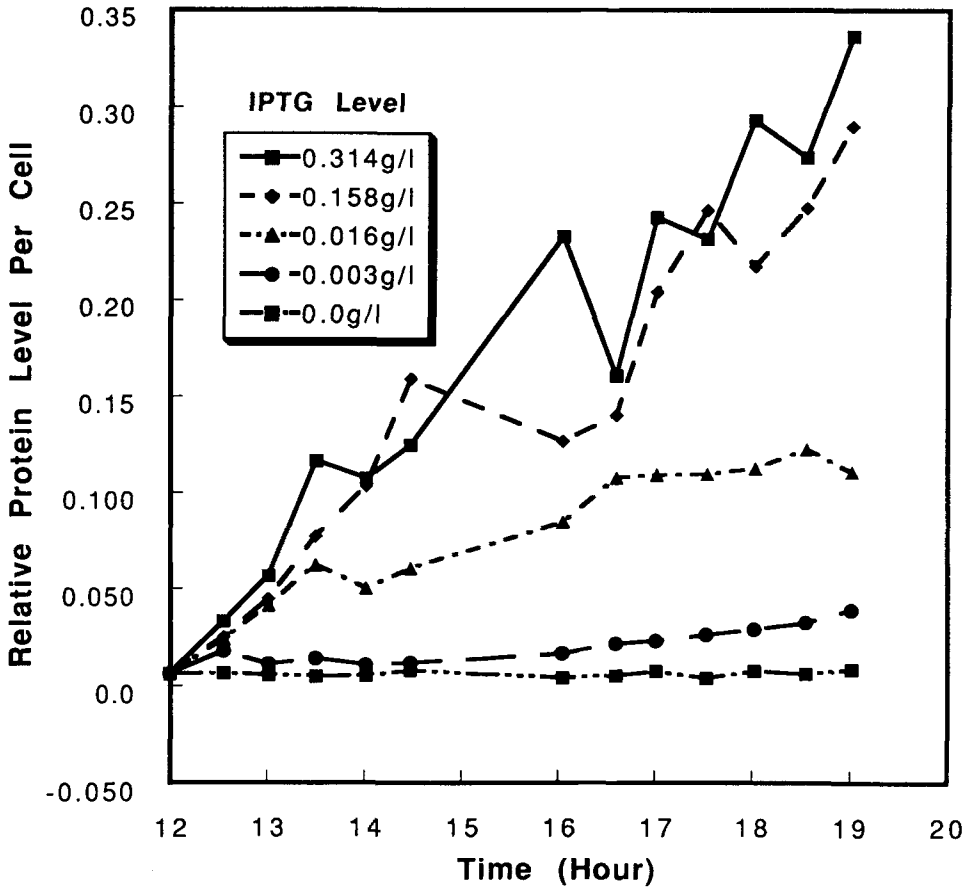

Figure 13. Relative protein level per cell mass at different IPTG concentrations.

Two extremes in foreign protein production also can be observed from Figure 3. The upper limit is modeled by a Monod-type expression and a lower limit is accomplished by a constant, f_{lo}, of Eq. (8). Model simulations of protein level agrees well with experimental data. Figure 13 shows the relative protein level in a cell from actual experiments. Figure 13 was constructed from the experimental data of Figures 3 and 6. The protein level in a cell increases rapidly with IPTG at a relatively lower IPTG concentration region, as shown in Figure 13. From the data without any IPTG in Figure 13, we see that the relative protein levels in a cell are almost constant with time, which implies that our experimental data are reliable.

Since our model can describe the batch process very well, the model was used to determine the optimal impulse injection of IPTG and amount levels. Our work can also be used to simulate fed-batch optimization studies, since the mathematical model of fed-batch systems has only a few additional terms due to the dilution effect of glucose and inducer inputs that can be accurately modeled. Optimal control theory can be applied to get optimal nutrient feeding rate and inducer feeding rate for fed-batch systems that maximize protein production.

This research was supported by the National Science Foundation under Grant No. BCS-8912259 and the Colorado Advanced Technology Institute through the Colorado Institute for Research in Biotechnology.

NOMENCLATURE

A	a constant defined in Eq. (7)
C_I	inducer level inside reactor, g/L
C_I^f	inducer level of feed, g/L
C_N	nutrient level inside reactor, g/L
C_N^f	nutrient level of feed, g/L
C_P	protein level inside reactor, g/L
C_P^O	relative protein level as an optical density of yellow *o*-nitrophenol
f_{lo}	a constant defined in Eq. (8)
$f_{\max}$	maximum protein production rate defined in Eq. (8)
$f_{\max}^O$	defined as $f_{\max} X_c/P_c$
k_1	shock rate constant defined in Eq. (5)
k_{11}	a constant defined in Eq. (5)
k_2	recovery rate constant defined in Eq. (6)
k_{22}	a constant defined in Eq. (6)
K_{C_N}	a constant defined in Eq. (2)
K_{IX}	a constant defined in Eqs. (5) and (6)
K_I	a constant defined in Eq. (8)
k_s	shock rate effect defined in Eq. (3)
k_r	recovery rate effect defined in Eq. (4)
P_c	defined as C_P/C_P^O
q_I	inducer feeding rate, L/h
q_N	nutrient feeding rate, L/h
R_f	foreign protein production rate, h^{-1}
R_f^O	modified foreign protein production rate, h^{-1}
R_R	recovery ratio defined in Eq. (2)
t	time, h

V culture volume, L
X cell mass, g/L
X_c defined as X/X^O
X^O optical density
Y growth yield coefficient (produced cell mass/consumed nutrient)
μ specific growth rate, h^{-1}
μ_{max} maximum specific growth rate, h^{-1}

References

1. Bailey, J. E., Ollis, D. F. 1986. Biochemical engineering fundamentals. 2nd edition. McGraw-Hill, New York.
2. Bentley, W. E. 1989. Effect of plasmid-mediated activity on bacterial metabolism and culture stability. Ph.D. Thesis. University of Colorado, Boulder, CO.
3. Bentley, W. E., Kompala, D. S. 1989. A novel structured kinetic modeling approach for the analysis of plasmid instability in recombinant bacteria cultures. Biotechnol. Bioeng. **33**: 49.
4. Childs, J., Villanueba, K., Barrick, D., Schneider, T. D., Stormo, G. D., Gold, L., Leitner, M., Caruthers, M. 1985. Ribosome binding site sequences and function. pp. 341–350 In: UCLA symposia on molecular and cellular biology, Vol. 30. Alan R. Liss, Los Angeles.
5. Georgiou, G. 1988. Optimizing the production of recombinant proteins in microorganisms. AICHE J. **34**: 1233.
6. Glick, B. R., Whitney, G. K. 1987. Factors affecting the expression of foreign proteins in *Escherichia coli*. J. Ind. Microbiol. **1**: 277.
7. Gold, L., Stromo, G. D. 1990. High-level translation initiation. pp. 89–93 In: Methods in enzymology, Vol. 185. Academic, London.
8. Ingraham, J. L., Maaloe, O., Neidhardt, F. C. 1983. Growth of the bacterial cell. Sinauer Associates, Sunderland.
9. Park, S., Ramirez, W. F. 1988. Optimal production of secreted protein in fed-batch reactors. AICHE J. **34**: 1550.
10. Park, T. H., Seo, J., Lim, H. C. 1989. Optimization of fermentation processes using recombinant *Escherichia coli* with the cloned *trp* operon. Biotechnol. Bioeng. **34**: 1167.
11. Peretti, S. W., Bailey, J. E. 1986. Mechanistically detailed model of cellular metabolism for glucose-limited growth of *Escherichia coli* B/r-A. Biotechnol. Bioeng. **28**: 1672.
12. Problem-solving software systems. 1987. IMSL Stat/Library User's Manual, Houston, Texas.
13. Shu, J., Shuler, M. L. 1989. A mathematical model for the growth of a single cell of *E. coli* on a glucose/glutamine/ammonium medium. Biotechnol. Bioeng. **33**: 1117.
14. Shuler, M. L. 1985. Invited review on the use of chemically structured models for bioreactors. Chem. Eng. Commun. **36**: 161.
15. Williams, F. M. 1967. A model of cell growth dynamics. J. Theor. Biol. **15**: 190.
16. Zabriskie, D. W., Arcuri, E. J. 1986. Factors influencing productivity of fermentations employing recombinant microorganisms. Enz. Microb. Technol. **8**: 706.